



Cancer cell-intrinsic function of CD177 in attenuating β -catenin signaling

Paige N. Kluz^{1,2} · Ryan Kolb³ · Qing Xie^{1,13} · Nicholas Borchering^{1,4} · Qi Liu⁵ · Yuewan Luo² · Myung-Chul Kim² · Linna Wang⁶ · Yinan Zhang⁷ · Wei Li² · Christopher Stipp^{8,9} · Katherine N. Gibson-Corley^{1,9} · Chen Zhao¹ · Hank H. Qi⁵ · Andrew Bellizzi^{1,9} · Andy W. Tao⁶ · Sonia Sugg^{9,10} · Ronald J. Weigel^{9,10} · Daohong Zhou¹¹ · Xian Shen¹² · Weizhou Zhang³

Received: 16 July 2019 / Revised: 27 January 2020 / Accepted: 30 January 2020 / Published online: 10 February 2020
© The Author(s), under exclusive licence to Springer Nature Limited 2020

Abstract

Aiming to identify immune molecules with a novel function in cancer pathogenesis, we found the cluster of differentiation 177 (*CD177*), a known neutrophil antigen, to be positively correlated with relapse-free, metastasis-free, or overall survival in breast cancer. In addition, *CD177* expression is correlated with good prognosis in several other solid cancers including prostate, cervical, and lung. Focusing on breast cancer, we found that *CD177* is expressed in normal breast epithelial cells and is significantly reduced in invasive cancers. Loss of *CD177* leads to hyperproliferative mammary epithelium and contributes to breast cancer pathogenesis. Mechanistically, we found that *CD177*-deficiency is associated with an increase in β -catenin signaling. Here we identified *CD177* as a novel regulator of mammary epithelial proliferation and breast cancer pathogenesis likely via the modulation of Wnt/ β -catenin signaling pathway, a key signaling pathway involved in multiple cancer types.

These authors contributed equally: Paige N. Kluz, Ryan Kolb, Qing Xie

Supplementary information The online version of this article (<https://doi.org/10.1038/s41388-020-1203-x>) contains supplementary material, which is available to authorized users.

✉ Xian Shen
13968888872@126.com

✉ Weizhou Zhang
zhangw@ufl.edu

¹ Department of Pathology, University of Iowa, College of Medicine, Iowa City, IA 52242-1109, USA

² Free Radical and Radiation Biology Program, University of Iowa, College of Medicine, Iowa City, IA 52242-1109, USA

³ Department of Pathology, Immunology and Laboratory Medicine, College of Medicine, University of Florida, Gainesville, FL 32610, USA

⁴ Medical Science Training Program, University of Iowa, College of Medicine, Iowa City, IA 52242-1109, USA

⁵ Department of Anatomy and Cell Biology, University of Iowa, College of Medicine, Iowa City, IA 52242-1109, USA

⁶ Department of Chemistry, Purdue University, West Lafayette, IN 47907, USA

Introduction

CD177 (also referred to as NB1, HNA-2a, or PRV1) is a glycosphosphatidylinositol (GPI)-linked extracellular membrane-bound protein that belongs to the Ly-6 family [1, 2]. *CD177* is a GPI-linked extracellular membrane

⁷ Department of Biology, College of Life Science, Nankai University, Tianjin 300071, China

⁸ Department of Biology, University of Iowa, College of Medicine, Iowa City, IA 52242-1109, USA

⁹ Holden Comprehensive Cancer Center, University of Iowa, College of Medicine, Iowa City, IA 52242-1109, USA

¹⁰ Department of Surgery, University of Iowa, College of Medicine, Iowa City, IA 52242-1109, USA

¹¹ Department of Pharmacodynamics, College of Pharmacy, University of Florida, Gainesville, FL 32610, USA

¹² Division of Gastrointestinal Surgery, The Second Affiliated Hospital of Wenzhou Medical University, Zhejiang 325035, China

¹³ Present address: Tumor Signaling and Transduction Laboratory, School of Basic Medical Sciences, Xinxiang Medical University, Xinxiang 453000, China

protein and has been shown to be expressed on the surface and in granules of human neutrophils and serves as a marker for myeloproliferative diseases [3, 4]. To study the physiological role of CD177, we have generated a CD177 knockout (*Cd177*^{-/-}) mouse model [5]. *Cd177*^{-/-} mice at 8 weeks of age exhibited slightly lower blood neutrophil, but they appear to have a normal function in clearance of bacterial infection and chemotaxis [5]. The roles of CD177 in solid cancers are largely unknown, though there is a correlation between loss of CD177 expression and poor prognosis in colorectal and gastric cancers [6, 7].

β -catenin is a member of the catenin family of proteins mainly involved in two distinct and relevant functions, with one being a structural protein involved in adherens junctions and the other as a Wnt-induced transcriptional co-activator where it plays an important role in development and tissue homeostasis [8]. β -catenin transcriptional co-activator activity is regulated by canonical Wnt signaling [9]. Cellular β -catenin largely exists in three pools, i.e., cytoplasmic, nuclear, or membrane bound. Cytoplasmic β -catenin is associated with the “destruction complex”, which phosphorylates β -catenin leading to its proteasomal degradation. Upon binding of a canonical Wnt ligand to its receptor, the destruction complex becomes associated with the membrane leading to β -catenin accumulation and nuclear localization. Membrane β -catenin forms a complex with E-cadherin at adherens junctions, together with p120-catenin and α -catenin that link to cytoskeleton microfilaments. There is strong evidence showing that membrane β -catenin can be used by Wnt signaling when E-cadherin or adherens junctions are genetically or chemically destroyed [10–13]. Furthermore, expression of E-cadherin in otherwise negative cells inhibits Wnt/ β -catenin-mediated transcription, thus supporting a role of E-cadherin/adherens junction in sequestering β -catenin to prevent its signaling [11, 14–18].

Dysregulation of β -catenin has a role in the development of several types of cancer, including breast cancer [19–22]. Wnt/ β -catenin signaling is important in all stages of normal mammary gland development through the regulation of mammary stem cells via a paracrine interaction between luminal epithelial cells and basal epithelial cells [19, 23–29]. Hyper-activation of β -catenin in the mammary gland leads to hyperplasia of mammary epithelial cells and often tumorigenesis when this pathway is dysregulated [30–37].

Here, we identified CD177 as a predictor for good prognosis in breast cancer and other types of cancer. We further identified an epithelial cell-intrinsic role of CD177 in tumor suppression that is associated with decreased β -catenin transcriptional activity.

Results

CD177 predicts RFS and MFS in breast cancer patients and other solid tumors

Using a published meta-data set of 3554 specimens [38], we generated a list of CD molecules whose RNA levels were correlated with relapse-free survival (RFS) in breast cancer (Table S1). *CD177* had one of the highest correlations between expression and RFS, higher than many other makers for immune cells with known anti-cancer functions, including those for NK cells (CD314/NKG2d, CD94), toxic T cells (CD8), macrophages (CD163), etc. (Supplementary Table 1, Fig. 1a hazard ratio (HR) = 0.62). *CD177* is also positively correlated with metastasis-free survival (MFS), in two well-established data sets, GSE2034 [39] ($n = 286$, Fig. 1b, Fig. S1A) and GSE2603 [40] ($n = 81$, Fig. S1B), irrelative of bone or lung metastasis (Fig. S1A, B). The positive correlation between *CD177* and RFS was true among all breast cancer subtypes (Fig. 1c and Supplementary Table 2).

Using Analysis of Illumina HiSeq expression data deposited in The Cancer Genome Atlas (TCGA) for 30 cancer types, we next checked if *CD177* expression was correlated with survival in other types as cancer. We found that *CD177* expression is positively correlated with survival in eight carcinomas (HR < 0.7 and Logrank $P < 0.05$; Fig. S1C and Supplementary Table 3), such as overall survival (OS) in cervical squamous cell carcinoma (HR = 0.44), RFS in lung squamous cell carcinoma (LUSC, HR = 0.60), and RFS in prostate cancer (HR = 0.5) (Fig. 1c and Supplementary Table 2).

CD177 is expressed in normal mammary epithelial cells but is reduced in breast cancer

As CD177 is a positive predictor for breast cancer, we determined whether CD177 is expressed on cells beyond neutrophils. Immunohistochemistry (IHC) images from Human Protein Atlas [54] revealed that CD177 is expressed on epithelial cells in cervical cancer, prostate cancer and LUSC (Fig. S1D–F). In breast cancer, *CD177* mRNA expression was reduced compared with normal tissues of 16-paired human breast cancer patients (Fig. 1d). Immunofluorescent staining revealed that CD177 was strongly expressed in the normal mammary epithelial cells but reduced in all paired cancer specimens (Fig. 1e; Fig. S2A). IHC staining for CD177, using a different monoclonal antibody (clone 4c4), of a tissue microarray (TMA) found CD177 staining in cancer cells, with lower levels of CD177 staining correlated with increased tumor stages (Fig. 1f, g).

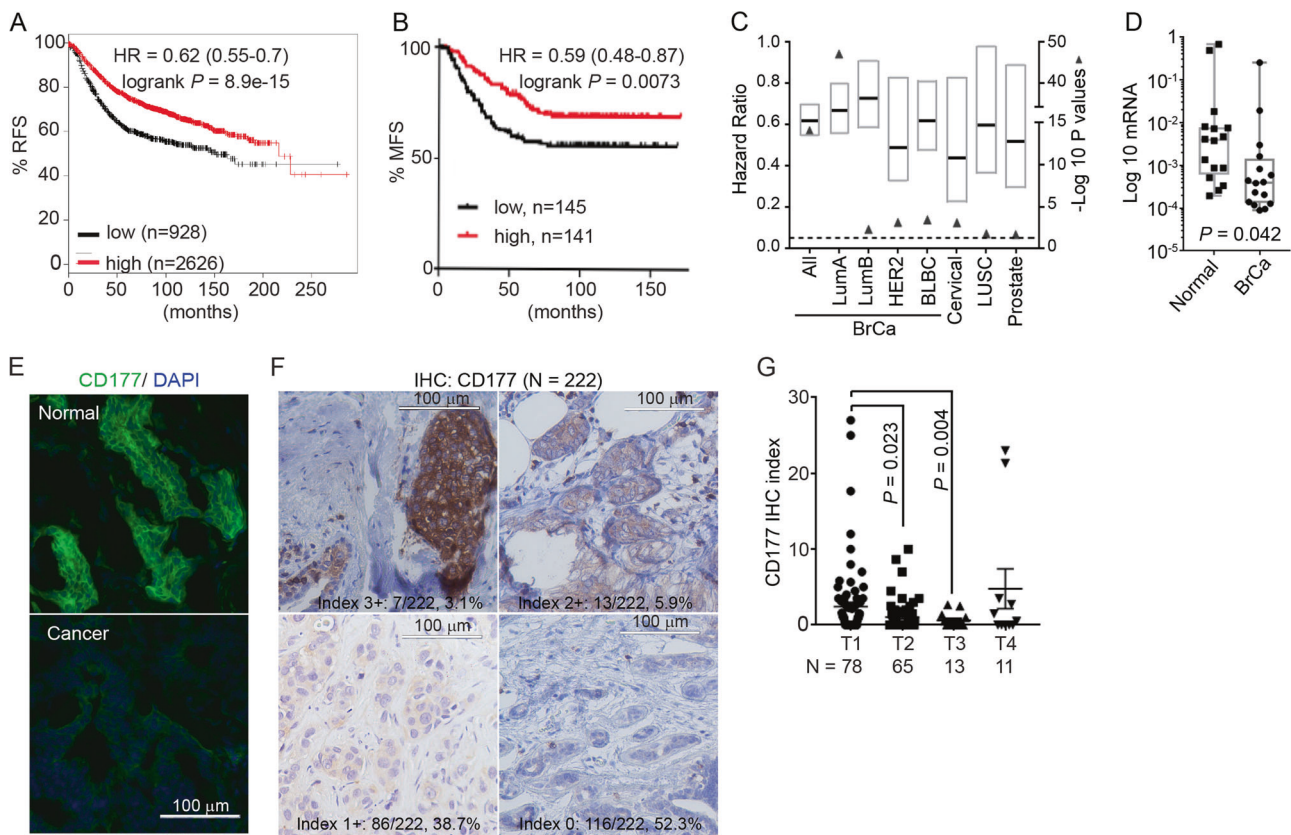


Fig. 1 *CD177* is commonly lost in invasive cancer and positively correlated with survival. **a** Correlation between *CD177* expression and relapse-free survival (RFS) in all breast cancer samples using an online KMPlot software including a total of 3554 breast cancer specimens. **b** Correlation between *CD177* expression and metastasis-free survival (MFS) in breast cancer among patient populations included in GSE2034 data set ($n = 286$). Logrank test was done to determine significance. **c** Correlation between *CD177* expression and RFS (breast cancer, BrCa; Lung squamous cell carcinoma, LUSC, and prostate cancer), and overall survival (OS, cervical cancer). BrCa data were generated using KMPlot software with samples separated by intrinsic subtypes (Luminal A, LumA; Luminal B, LumB; HER2⁺; basal-like breast cancer, BLBC). Cervical, LUSC, and prostate data are from TCGA Illumina HiSeq level 3 data. Graph represents the hazard ratio (black bar) and range (box) with the $-\text{Log}_{10}$ Logrank P value (closed

triangle). Dashed line is $-\text{Log}_{10}(0.05)$. N numbers for each group is presented in Table S2. **d** *CD177* log₁₀ mRNA level in breast cancer and paired normal tissue. $n = 16$, paired t test. **e** Representative immunofluorescent staining for *CD177* in human breast cancer specimen and paired normal tissue ($n = 6$ pairs, also Fig. S2A). **f** Representative IHC staining for *CD177* of a tissue microarray of 222 human breast cancer samples. Samples were scored using index of 0–3+ based on the intensity of *CD177* staining and percentage of positivity. The intensity scores and number/percentages are indicated. **g** *CD177* IHC index for samples from **f** separated by tumor stage. IHC index was calculated by the following formula: Intensity index \times percentage $\times 10$. One-way ANOVA was used to determine significance with adjusted P values indicated. Only samples with traceable tumor stage information were shown ($n = 167$). Also see Supplementary Table S1–S3 and Figs. S1–S2.

Most breast cancer cell lines had significantly decreased *CD177* mRNA levels compared with non-fully transformed HMLE mammary epithelial cells (Fig. S2B). These cells had nearly undetectable expression of *CD177* by western blot or surface expression by flow cytometry under monolayer culture. However, when mouse mammary breast cancer 67NR, prostate cancer PC3, lung cancer H146 and a tamoxifen-resistant MCF-7 (MCF-7-R) cell lines were grown in non-adherent conditions, *CD177* protein was found on the cell surface by flow cytometry (Fig. S2C–E).

To determine whether *CD177* locus is commonly mutated, deleted or has promoter methylation, we utilized cBioPortal data set [41, 42] and found no recurrent mutations or chromosomal deletions related to *CD177* locus. We

also mined TCGA datasets for invasive breast cancer and found no significant correlation between promoter methylation and *CD177* expression in either breast cancer samples or normal breast tissues, suggesting that *CD177* expression in breast cancer may not be regulated by promoter methylation (Fig. S2F).

CD177 deficiency induces hyperproliferation of mammary epithelial cells

As we observed a common loss of *CD177* in human breast cancer, we sought to further study the physiological function of *CD177* in the mammary gland to better understand the role of *CD177* in mammary epithelial

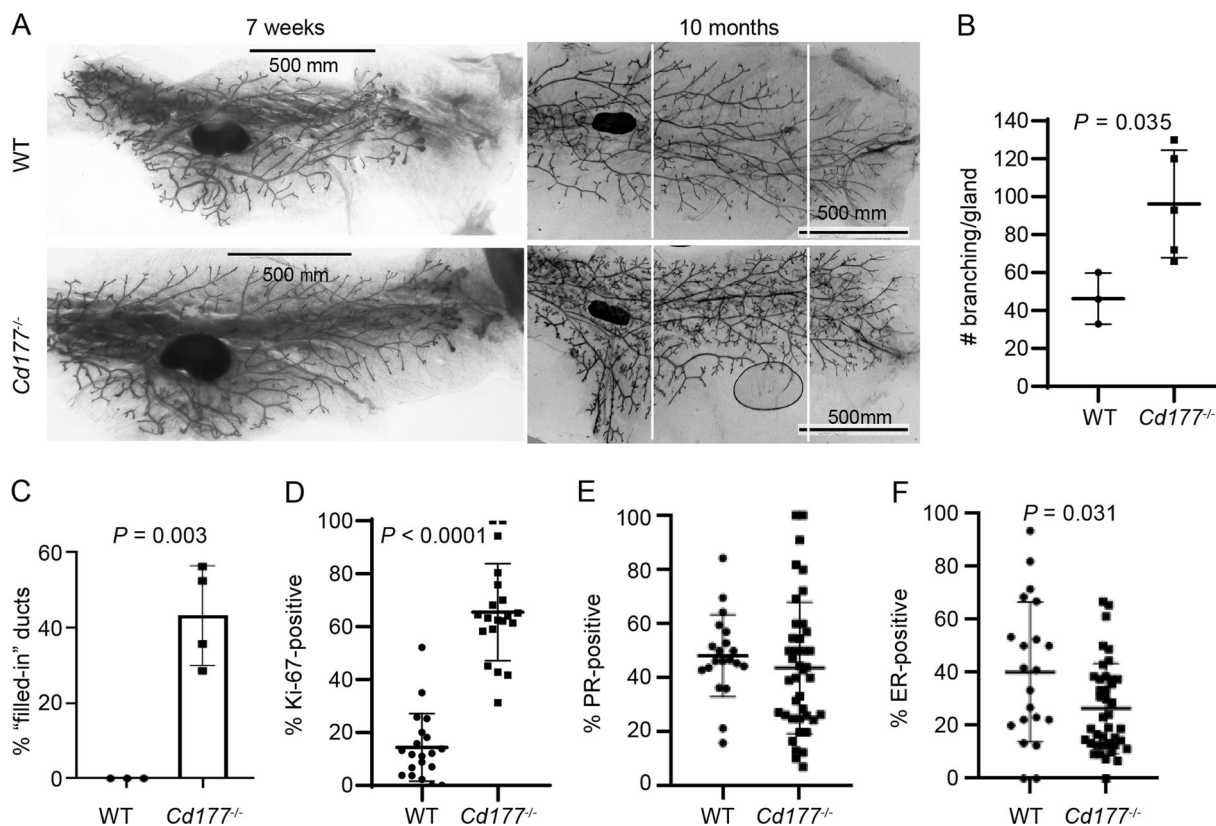


Fig. 2 CD177 deficiency leads to proliferative mammary epithelial cells. **a** The No. 4 mammary glands from the indicated mice were collected at 7 weeks (left panels) and 10 months (right panels) of age. The number of branches between the white lines was counted. **b** Graph depicts the number of branches from **a** from the indicated mice. Significance was determined with Student's *t* test ($n = 3$ WT, $n = 5$ *Cd177*^{-/-}). **c** Number of filled ducts was counted from age-matched mice at 10 months ($n = 3$ WT, $n = 5$ *Cd177*^{-/-}), based on H&E images

shown in Fig. S3A. **d** Percentages of Ki-67-positive cells was calculated from mammary epithelial cells of age-matched mice at 10 months ($n = 3$ WT, $n = 5$ *Cd177*^{-/-}, 5–10 ducts counted per gland), based on IHC shown in Fig. S3B. **e**, **f** Percentages of PR- **e** or ER- **f** positive cells was calculated from mammary epithelial cells of age-matched mice at 10 months ($n = 2$ WT, $n = 4$ *Cd177*^{-/-}, 10 ducts counted per gland), based on IHC shown in Fig. S3C. Also see Fig. S3.

cells. We examined the physiological function of CD177 in the mammary gland using *Cd177*^{-/-} mice [5]. At 7 weeks, there was no discernable difference in mammary glands of knockout mice compared with wild-type littermates (Fig. 2a). However, mammary glands from 10 month old *Cd177*^{-/-} mice exhibited significantly increased side branching and ductal structures (Fig. 2a, b). Hematoxylin and Eosin staining revealed many mammary duct structures with loss of luminal architecture and multiple layers of epithelial cells (Fig. S3A, black arrows). This phenotype was not found in the wild-type (WT) littermates (Fig. S3A, Fig. 2c). The mammary epithelium from the *Cd177*^{-/-} mice had increased proliferation indicated by Ki-67 IHC (Fig. 2d, Fig. S3B, upper panels). *Cd177*^{-/-} mice exhibited similar nuclear progesterone receptor (PR, Fig. 2e, Fig. S3C, left) and slightly decreased nuclear estrogen receptor (ER, Fig. 2f, Fig. S3C, right), suggesting the hormone-independent proliferative phenotype within *Cd177*^{-/-} mammary epithelium. This suggests that CD177-deletion promotes the

expansion of mammary epithelial cells, a prerequisite for breast cancer development.

Normal mammary ducts from both *Cd177*^{-/-} and WT mice contained a single layer of keratin (Krt) 5-positive basal cells and Krt-8-positive luminal cells, whereas the filled mammary ducts from *Cd177*^{-/-} mice had multiple layers of basal and luminal cells (Fig. S3B, lower panels). We observed no difference in the percentage of Krt-5- or Krt-8-positive cells in mammary glands from *Cd177*^{-/-} mice compared with WT littermates (Fig. S3D, E). These data indicate that CD177 deficiency leads to an increase in both luminal and basal epithelial cells while maintaining their ratio.

CD177 is a critical regulator for mammary tumorigenesis

To study the role of CD177 in breast cancer, we stably overexpressed human CD177 in human breast cancer cell lines, including MCF-7 (luminal, Fig. 3a) and SKBR3

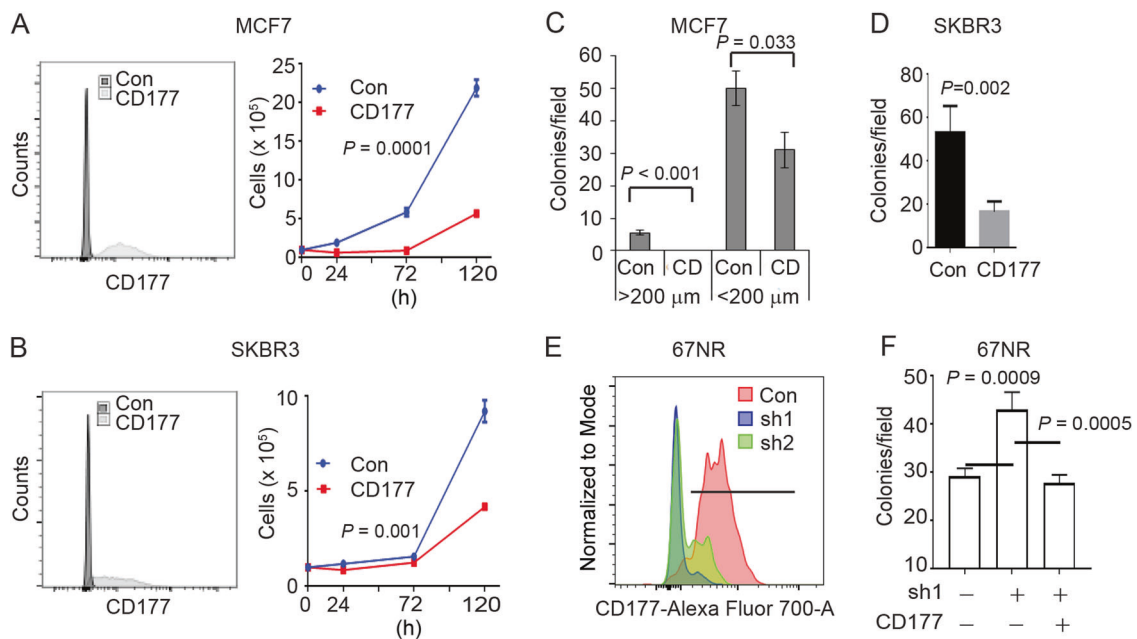


Fig. 3 CD177 suppresses breast cancer cell growth and colony formation. **a, b** The indicated cells stably expressing CD177 or GFP (con) vector were purified by surface CD177 staining and flow cytometry. Expression of surface CD177 was determined by flow cytometry (left panels) and monolayer cell growth curves were shown (right panels). Two-way ANOVA was done to determine significance ($n = 3$). **c, d** Three-dimensional soft agar assay for MCF-7 **c** and SKBR3 **d** expressing CD177 (CD) or GFP (Con). Graphs depict the average number of colonies per microscopy field \pm s.d. At least three fields per sample were counted. Students *t* test was done to determine

significance ($n = 3$). 200 μ m in **c** defines the colony size. **e** 67NR cells were selected for stable expression of CD177 shRNA following lentivirus transduction from two independent shRNAs. Graph depicts the surface CD177 expression determined by flow cytometry. **f** Three-dimensional soft agar assay for 67NR control or sh1 cells from **e** transfected with human CD177 as indicated. Graph depicts the average number of colonies per microscopy field \pm s.d. At least three fields per sample were counted. One-way ANOVA was used to determine significance. Also see Fig. S4.

(HER2⁺, Fig. 3b). Overexpression of CD177 in MCF-7 and SKBR3 cells reduced monolayer growth (Fig. 3a, b) and soft agar colony formation (Fig. 3c, d). In concordance, silencing *Cd177* in 67NR (murine mammary carcinoma) cells by shRNA (Fig. 3e, Fig. S4A) resulted in an increase in the number of soft agar colonies, which was reversed when CD177 was reconstituted (Fig. S4B, Fig. 3f).

To confirm the role of CD177 as a cancer cell-intrinsic tumor suppressor, we orthotopically injected *CD177*-overexpressing MCF-7 or MDA-MB-231 cells into immunodeficient NOD-*scid* IL2R γ^{null} (NSG) mice. Tumor growth was significantly suppressed relative to control tumors for both cell lines (Fig. 4a, b). Likewise, silencing *Cd177* in 67NR cells (Fig. 3e, Fig. S4A) resulted in the increased tumor growth compared to 67NR control cells (Fig. 4c).

We also examined the role of CD177 in an oncogene-induced mammary tumor model. We crossed *Cd177*^{-/-} mice [5] with *MMTV-ErbB2*-transgenic (tg) mice to produce *MMTV-ErbB2/Cd177*^{+/-} or *MMTV-ErbB2/Cd177*^{-/-} littermate progeny. The *MMTV-ErbB2/Cd177*^{-/-} mice did not show difference in first tumor onset (Fig. S4C), but had increased tumor multiplicity compared with *MMTV-ErbB2/Cd177*^{+/-} littermates (Fig. 4d, $P = 0.023$); 41% of the *MMTV-ErbB2/Cd177*^{-/-} mice but only 4.5% of the *MMTV-*

ErbB2/Cd177^{+/-} mice had more than three tumors (Fig. 4e). Surface expression of CD177 was verified in a small percentage of cancer cells in *MMTV-ErbB2/WT* mice, indicative of reduced CD177 expression in cancer (Fig. S4D, Fig. 4f). As expected, no CD177 was observed in tumors from *MMTV-ErbB2/Cd177*^{-/-} mice (Fig. 4f). Unlike the cell line data (Fig. 3a, b) or within mammary glands (Fig. 2), there was no significant increase in Ki-67-positive cells in these tumors (Fig. S4E, F), suggesting that tumors evade CD177-mediated suppression of proliferation at late stages likely by downregulation of surface CD177 (Fig. 4f).

CD177 expression is associated with decreased β -catenin activity

As nothing is known related to CD177-mediated signaling transduction in cancer, we performed datamining of the TCGA invasive breast cancer (BrCa) data set. We correlated *CD177* expression with known biological pathways using gene set enrichment analysis (GSEA) [52], comparing BrCa samples with low versus high *CD177* expression. We found that the low expression of *CD177* was correlated with the enrichment of Wnt and β -catenin

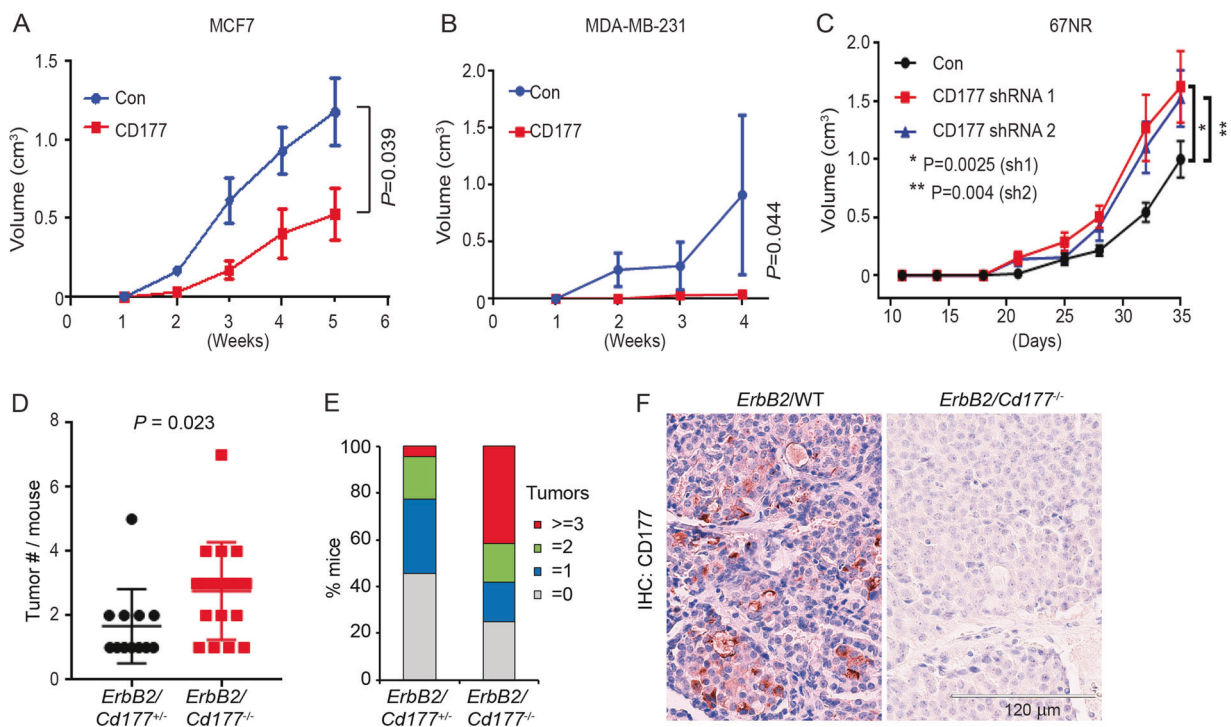


Fig. 4 CD177 suppresses tumorigenesis in a cancer cell-intrinsic manner. **a**, **b** MCF-7 **a** or MDA-MB-231 **b** cells stably expressing CD177 or control vector (con) were implanted into the number 4 mammary glands of NSG mice and tumor volume was monitored. Graph depicts the average tumor volume \pm s.e.m. Two-way ANOVA was used to determine significance ($n=4-6$). **c** 67NR cells stably expressing CD177 shRNA1, shRNA2, or control 67NR cells from Fig. 3e were implanted into the No. 4 mammary fat pad of Balb/c mice and tumor volume was monitored. Graph depicts the average tumor volume \pm s.e.m. Two-way ANOVA was used to determine

significance. **d**, **e** MMTV-ErbB2/Cd177^{+/-} and MMTV-ErbB2/Cd177^{-/-} mice were monitored for tumor development. Mice were killed when the largest tumor reached 2 cm and the number of tumors per mice was counted. Graph depicts the number of tumors per mouse (**d**, only tumor-bearing mice were shown) or the percent of mice with the indicated number or tumors (**e** all mice were shown) from MMTV-ErbB2/Cd177^{+/-} and MMTV-ErbB2/Cd177^{-/-}. **f** Representative IHC images for CD177 in tumors from MMTV-ErbB2/WT and MMTV-ErbB2/Cd177^{-/-} mice. Also see Fig. S4.

signaling (Fig. 5a). Similar results were found in several other major cancer subtypes including the TCGA LUSC, colon adenocarcinoma and rectal adenocarcinoma (READ) (Fig. 5b), where CD177 expression was observed either in corresponding cancer specimens (Fig. S1F) or known in literature [6]. Next generation RNA sequencing also revealed that *Cd177*-deficiency led to decreased expression of Wnt/ β -catenin-targeted genes within *ErbB2*-induced tumors from Fig. 4d-f (Supplementary Table 4, Fig. 5c) and further validated by real-time PCR (Fig. 5d, Fig. S5A). We have shown before that human breast cancers rarely have nuclear β -catenin [55], in agreement with previous publications using clinical approved IHC protocols [37, 56]. Using an antibody that specifically recognizes active β -catenin, we did not find significant nuclear β -catenin staining on tissue sections of these *ErbB2*-induced tumors, either within *Cd177*^{+/-} or *Cd177*^{-/-} genotypes. Staining of normal glands from Fig. 2a, we found that *Cd177* deficiency led to a significant increase in nuclear β -catenin staining of mammary glands from 10-month-old mice, preferably within the basal layer of mammary epithelium (Fig. 5e, f), in agreement

with the critical role of β -catenin in basal mammary stem cells.

We also determined whether CD177 regulates the β -catenin-mediated transcription using a dual-luciferase TOPflash assay [45]. We found that knockdown of *Cd177* in 67NR cells increased basal level of β -catenin transcriptional activity with slight but not significant increase with Wnt3a treatment (Fig. 5g). In H146 cells with intrinsic CD177 expression (Fig. S2C, E), silencing CD177 by siRNA (Fig. S5B) significantly increased both basal and Wnt3a-induced β -catenin transcriptional activity compared with control cells (Fig. S5B). Further supporting the sufficiency of CD177 in attenuation of β -catenin activity, overexpression of CD177 in the CD177 negative MDA-MB-436 cells significantly reduced Wnt3a-mediated β -catenin activity (first two open bars in Fig. 5h, S5C). As we have seen silencing CD177 in 67NR cells resulted in the increased in vitro (Fig. 3f) and in vivo (Fig. 4c) tumor growth, we further silenced β -catenin in 67NR sh1 cells to determine the causative role of β -catenin downstream of CD177-deficiency. We achieved

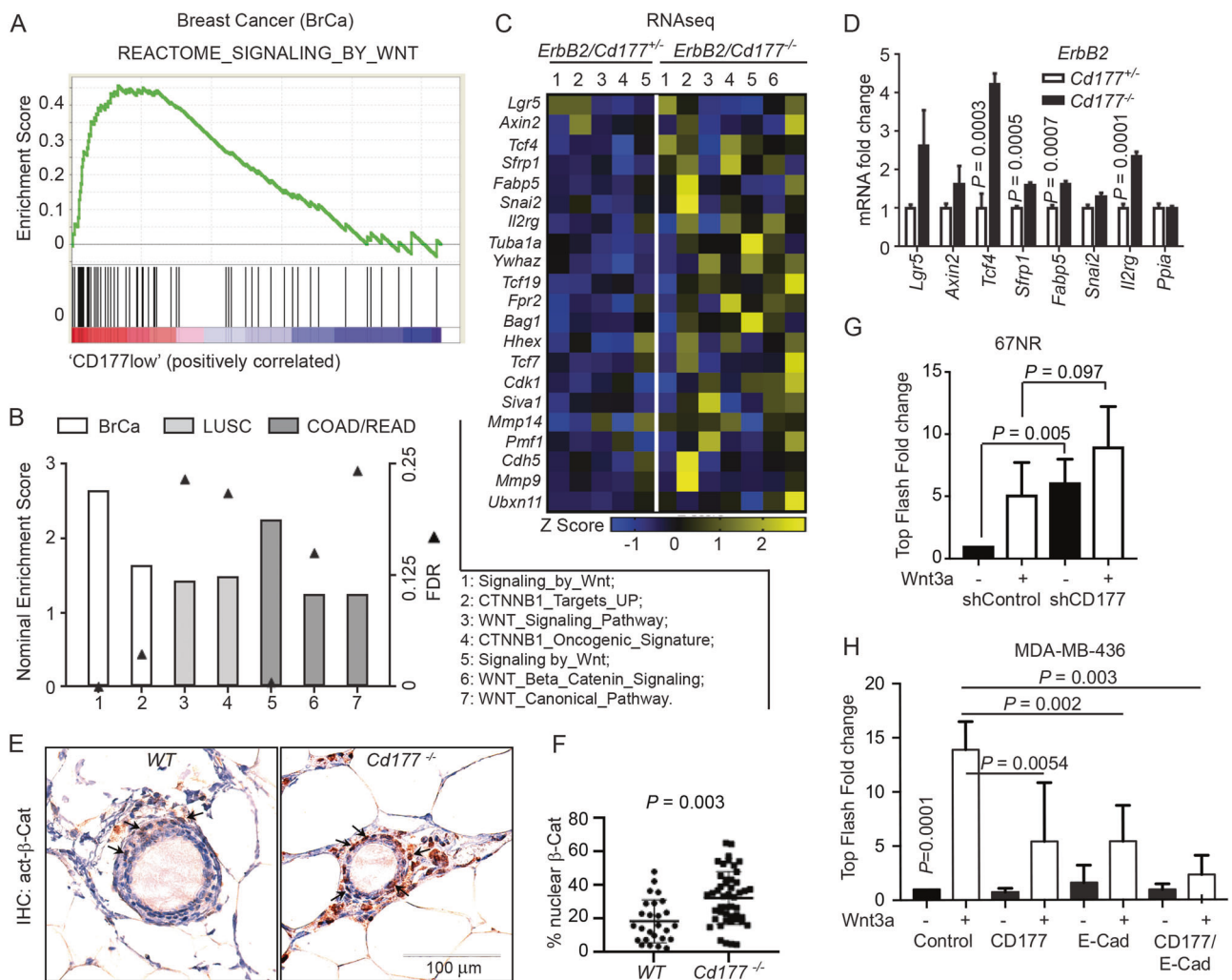


Fig. 5 **CD177 attenuates the canonical Wnt/ β -catenin signaling.** **a, b** GSEA showing activation of Wnt/ β -catenin pathways in $CD177^{low}$ cohorts of human cancers, including human breast cancer samples (BrCa; GSE2034, 19 $CD177^{low}$ versus 19 $CD177^{high}$ cancer specimens), lung squamous cell carcinoma (LUSC; TCGA), colon adenocarcinoma (COAD; TCGA), and rectal adenocarcinoma (READ; TCGA). Cancer specimens were separated into high versus low $CD177$ expressing groups (BrCa: low 19 vs high 19; LUSC: low 98 vs high 98; COAD: low 33 vs high 33; READ: low 15 vs high 15). Graph depicts the net enrichment score (bar) and false discovery rate (FDR, solid triangle) for the indicated gene sets in the $CD177$ low groups. **c** RNAseq was performed using tumor RNAs collected from *MMTV-ErbB2/Cd177^{+/−}* and *MMTV-ErbB2/Cd177^{−/−}* mice used in Fig. 4d (5 and 7, respectively, Table S4). Heatmap depicting Z scores for the expression of β -catenin-regulated genes, defined by GSEA Wnt/ β -catenin-regulated gene signatures in cancer cells, including combined genes from the following GSEA gene sets: Go_Canonical_Wnt_Signaling_Pathway; Go_Wnt_Signaling_Pathway; Biocarta_Wnt_Pathway. **d** Real-time PCR verifying the mRNA expression of several genes in tumors from the indicated mice. Graph depicts the average mRNA expression relative to *Ppia* as a fold change compared with *WT* group \pm s.d. Student's *t* test was done to determine significance ($n = 3$ from different tumors). **e, f** Representative IHC images **e** and percentages of active nuclear β -catenin **f** positive cells were calculated from mammary epithelial cells of age-matched mice at 10 months ($n = 2$ *WT*, $n = 3$ $CD177^{-/-}$, 12–17 ducts counted per gland). **g** TOPflash dual-luciferase assay for 67NR cells stably expressing CD177 shRNA (Fig. 3e) grown in non-adherent conditions in polyHEMA coated plates. Cells were then treated with or without 400 ng/mL recombinant Wnt3a for 24 hr. Graph depicts the average firefly luciferase intensity as a fold change compared with untreated control \pm s.d. One-way ANOVA was used to determine significance. $n = 6$ for all experiments. **h** TOPflash dual-luciferase assay for β -catenin activation in MDA-MB-436 cells transfected with pcDNA3.1 empty vector (control), CD177 and pcDNA3.1, E-cadherin and pcDNA3.1 or both E-cadherin and CD177, treated with or without 400 ng/mL recombinant Wnt3a for 24 hr. Graph depicts the average firefly luciferase intensity as a fold change compared with untreated control \pm s.d. One-way ANOVA was used to determine significance ($n = 6$ for all experiments). **g, h** black bars, no treatment; white bars, 400 ng/ml of Wnt3A treatment. Also see Fig. S5.

>90% reduction of β -catenin protein level in 67NR sh1 cells (Fig. S5D, right panels), which led to significantly reduced colony growth from the 67NR sh1 cells (Fig. S5D, left panels).

CD177 indirectly interacts with β -catenin

To gain mechanistic understanding how CD177, a GPI-linked extramembrane protein without a transmembrane

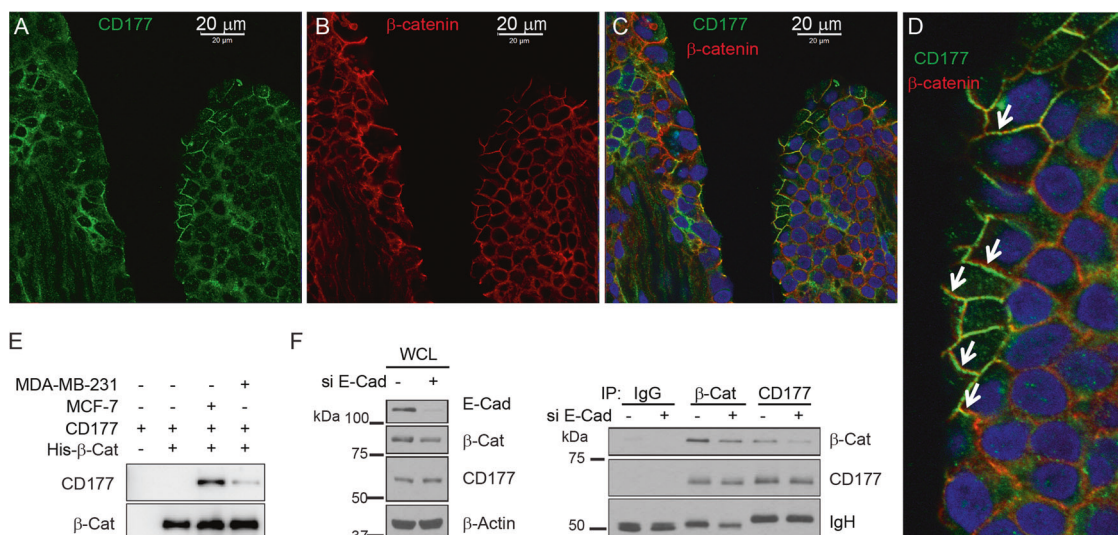


Fig. 6 CD177 indirectly interacts with β -catenin. **a–d** Normal human breast tissues were stained with anti-CD177 (**a**: green, clone 4c4) and anti- β -catenin (**b**: red). Representative confocal images are shown as individual colors and an overlay **c** with nuclear DAPI staining (blue). **d** Enlarged merged image from **c** with white arrows indicating areas where the two signals are parallel. **e** 1 μ g of FC-fusion CD177 and His-Tag full-length β -catenin, both purified from HEK293T cells, were incubated using RIPA buffer, with or without

the presence of 1 mg of cell lysates from MCF-7 or MDA-MB-231 cells. Ni-NTA agarose was used to pull down His- β -catenin complex, following with SDS-PAGE and Western Blotting. Also see Fig. S6D ($n = 2$). **f** Immunoprecipitation of β -catenin or CD177 from MCF-7-R cells transfected with E-cadherin siRNA. IP using non-immunogenic IgG was used as a control. Immunoblotting of whole-cell lysates (WCL, left) and IP (right) for E-cadherin, β -catenin, CD177, β -actin, and/or IgG heavy chain (IgH) are shown ($n = 2$). Also see Fig. S6.

domain, regulates intracellular β -catenin activity, we further characterized the molecular nature of CD177 on cancer cells. CD177 was found to be expressed on the membrane (Fig. S2C by surface flow cytometry, Fig. S6A by immunofluorescence staining), indicative of physiological membrane localization. Using the confocal microscope, we further found that both CD177 (Fig. 6a: green) and β -catenin (Fig. 6b: red) were localized at sites of cell–cell contact (Fig. 6a–c) within normal human mammary glands, whereas control IgGs did not yield any fluorescence signal (Fig. S6B). The two signals were mostly in parallel with each other (Fig. 6d, white arrows), indicating the two are likely at the opposite sides of the plasma membrane. As extracellular CD177 does not have a transmembrane domain and β -catenin is an intracellular protein, we reasoned the transmembrane E-cadherin may mediate the interaction since both E-cadherin and β -catenin belong to the protein complex involving adherens junctions. We identified co-localization between CD177 and E-cadherin along the plasma membrane of normal human mammary ducts (Fig. S6C). We further combined FC-fusion CD177 recombinant protein with His-Tag full-length β -catenin, both purified from HEK293T cells, and did not detect any interaction by pull down assays (Fig. 6e and Fig. S6D, first two lanes). Co-incubation with cell lysates from MCF-7 (E-cadherin positive), MDA-MB-231 (E-cadherin negative) (Fig. 6e), or HEK293T (Fig. S6D) induced the interaction between CD177 and β -catenin. We further used an anti-E-

cadherin antibody to deplete E-cadherin protein from HEK293T lysate, using an IgG or non-relevant anti-transmembrane protein DSG2 as negative controls (Fig. S6E). Depletion of E-cadherin did not influence the interaction between CD177 and β -catenin (Fig. S6D). We also depleted E-cadherin by siRNA with a 90% silencing efficiency in MCF-7-R cells (Fig. 6f) without altering the levels of endogenous CD177 and β -catenin (Fig. 6f). Same lysates were subject to co-immunoprecipitation (co-IP) where anti- β -catenin pulled down both β -catenin and CD177 regardless of E-cadherin expression (Fig. 6f, right panels). The reciprocal co-IP of CD177 showed similar results (Fig. 6f). CD177-dependent suppression of β -catenin activity was independent of E-cadherin in an E-cadherin-negative MAM-436 cells (Fig. 5h). These data indicate that CD177 forms a complex with β -catenin indirectly along the plasma membrane.

Discussion

We identified a novel function of CD177 as a tumor-suppressive protein and biomarker for predicting patient outcomes in breast and other types of cancer. The expression of CD177 is decreased in paired invasive cancers as well as more advanced tumors, which agrees with the general loss of tumor suppressors during cancer development. CD177 expression also predicts a good patient

outcome in breast cancer and other cancer types. Although the loss of CD177 alone was insufficient to induce tumorigenesis, it did induce hyperproliferation of mammary epithelial cells. Mammary ducts from 10-month-old *Cd177*^{-/-} mice exhibited multiple layers of epithelial cells with some filled ducts, a phenotype observed in the early stages of tumorigenesis and puberty. This resembles the activation of β -catenin in the mammary gland that leads to hyperproliferation of the mammary epithelial cells and adenocarcinoma [30, 31]. Nuclear β -catenin is also elevated within the mammary epithelial cells from 10-month-old *Cd177*^{-/-} mice relative to *WT* mice.

We also found that CD177 forms a complex with β -catenin, suppressing Wnt-induced β -catenin transcriptional activity. Though constitutive activation of Wnt signaling leads to adenocarcinoma in aged mice, *Cd177*^{-/-} mice did not develop spontaneous carcinomas. β -catenin is a known tumor promotor in several other types of cancer where CD177 is a good prognosis marker such as cervical [57–59], prostate [60, 61], and LUSC [62, 63]. CD177 may act as a tumor suppressor in these cancers by attenuating β -catenin signaling similar to breast cancers.

We have made a long-term commitment to determine a transmembrane protein that potentially mediates the interaction between extracellular CD177 and intracellular β -catenin. The apparent E-cadherin fails to fulfill this function. Several attempts using mass spectrometry also failed to identify a membrane protein that bridges CD177 and β -catenin; whereas the search is ongoing, it is important to add CD177 as a negative regulator of β -catenin activity. In summary, our results support a model where CD177 indirectly interacts with β -catenin at the plasma membrane independently of E-cadherin, preventing β -catenin activation. This is in agreement with bioinformatics analysis where CD177 is a good prognostic factor in various cancer types.

Materials and methods

Murine models

All animal experiments were in accordance with University of Iowa IACUC guidelines. NOD-*scid* IL2R γ ^{null} (NSG) (Jackson laboratory, Bar Harbor, Maine) mice were implanted with subcutaneously with estradiol pills (Innovative Research of America, Sarasota, FL). Three days later, 1×10^6 MCF-7 CD177-myc or green fluorescent protein (GFP) cells in 50% Matrigel (Corning, Corning NY)/phosphate-buffered saline (PBS) were orthotopically transplanted. In all, 2×10^6 MDA-MB-231-overexpressing CD177-myc or GFP cells in 50% Matrigel (Corning, Corning NY)/PBS were orthotopically transplanted. Balb/C

female 6-week-old mice were injected with 2.5×10^5 67NR cells or 67NR cells expressing control or CD177 shRNAs (sh1 or sh2) in 50% Matrigel (Corning). All cells were transplanted into the number four mammary fat pad. For the syngeneic orthotopic transplant tumor model, 6-week-old Balb/C female mice were obtained from Charles River Laboratories (Burlington, MA). Tumor growth and development was monitored by external palpations and measured using calipers. Tumor volume was calculated as length \times width² \times 0.502. *MMTV-ErbB2* mice were crossed with *CD177*^{-/-} mice to generate *MMTV-ErbB2/WT*, *MMTV-ErbB2/CD177*^{+/-} and *MMTV-ErbB2/CD177*^{-/-} littermates. All comparisons between *WT* and *CD177*^{-/-} as well as those between *MMTV-ErbB2/CD177*^{+/-} and *MMTV-ErbB2/CD177*^{-/-} were made between littermates or aged-related mice. Tumor-free survival was determined by recording the date the mice first had palpable tumors 2 weeks in a row. All mice were terminated when their largest tumor reached 2 cm in diameter or when they reached 600 days old. Tumor multiplicity was determined by counting the number of individual tumors at the time when mice were terminated. With a fixed power of 0.8, for transplant models, we expect a variation of 0.5 standard deviation and a twofold change, giving 5–6 per group of animals; for spontaneous models, we expect a variation of one standard deviation and a twofold change, giving 17–18 per group of animals. Randomization and double-blinded measurements were performed for all transplantation animal experiments.

Survival analysis

Kaplan–Meier survival curves were made using GraphPad Prism software (GraphPad Software Inc., San Diego, CA) from publicly available data sets. RFS based on RNA expression of CD molecules were generated using data from a published meta-data set of 3554 breast cancer specimens and the KMplot online tools (KMplot.com) [38]. MFS curves were generated using data from GEO Dataset GSE2034 [39] ($n = 286$) and GSE2603 [40] ($n = 81$). Level 3 Illumina RNAseq data were obtained from the TCGA for 30 cancer types from the cBioPortal [41, 42]. HRs and *P* values for survival based on *CD177* expression were determined using Cox's proportional hazards model.

Cell lines, transfection, and transduction

SKBR3, MDA-MB-231, MDA-MB-436, HEK293T, and MCF-7 cells were obtained from ATCC and maintained in Dulbecco's Modified Eagle Medium (DMEM) (Life Technologies, Waltham, MA) with 10% fetal bovine serum (FBS). HMLE cells were provided by Dr. Jing Yang (University of California, San Diego) and maintained in F12

media (Life Technologies) supplanted with 10% FBS, 0.1% insulin, 2 µg/ml hydrocortisone, and 10 ng/ml epithelial growth factor. H146, obtained from ATCC, and 67NR, 168FARN, and 4TO7 cells were maintained in Roswell Park Memorial Institute 1640 media supplemented with 10% FBS. Human colon epithelial cells were obtained from Dr. Jerry Shay (University of Texas Southwestern) and cultured in DMEM with 10% FBS. Human mammary epithelial cell line (AG11132) was obtained from Coriell Institute for Medical Research (Camden, NJ), and cultured using mammary epithelial cell growth medium complete medium (Lonza, Basel, Switzerland). MCF7-R cells [43] were from Dr. Marc Lippman at the National Cancer Institute and cultured using DMEM (Life Technologies, Waltham, MA) with 10% FBS. For non-adherent culture of 67NR and H146 cells, plates were coated with poly 2-hydroxyethyl methacrylate (polyHEMA; Sigma Aldrich, St Louis MO) 12 mg/ml of 95% ethanol and allowed to evaporate. In all, 2×10^5 cells per ml were plated and cultured for 48 h. ATCC cells were used within 5–6 generations and other cells were tested for mycoplasma using Plasmotest-Mycoplasma Detection (InvivoGen, San Diego, CA). For CD177 shRNA, Lentivirus containing shRNA sequences were packaged in HEK293T cells and media containing packaged virus was collected. 67NR cells were incubated with media containing the packaged shRNA lentivirus for 24 h and stable cells lines expressing the CD177 shRNA were generated by selection of transduced cells with 4 µg/ml puromycin (Thermo Fisher Scientific). The mouse CD177 shRNA's targeting sequences: Sh1 5'-GCCAAGACTTGATAATGCTCC-3'; Sh2 5'-ACC CAGGCGATTGGGACCTTG-3' were used to silence CD177 in 67NR cells. For soft agar colony assay, 5×10^4 cells were suspended in 0.4% agarose/media mixture and plated on top of solidified 0.8% agarose/media mixture. Colonies were cultured for 2 weeks and counted. For monolayer growth curves, 1×10^5 cells were plated and counted at 24, 72, and 120 h.

Cell lysates, immunoprecipitation, and immunoblots

For membrane and cytosolic fractionation, we followed our previously described protocol [44].

For immunoprecipitation, 1 mg of cell lysate was incubated with 1 µg/mL of antibodies at 4 °C overnight. Immunocomplex was precipitated using protein A or G sepharose beads (Thermo Fisher Scientific). Sepharose beads were resuspended in SDS loading buffer and separated by sodium dodecyl sulfate polyacrylamide gel electrophoresis (SDS-PAGE) and visualized by western blotting. For in vitro pull down assay, 1 µg of FC-fusion CD177 (14501-H02H, SinoBiological, Beijing, China) and His-Tag full-length β-catenin (11279-H20B, SinoBiological), both purified from HEK293T cells, were incubated

using radioimmunoprecipitation assay buffer, with or without the presence of 1 mg of cell lysates from MCF-7 or MDA-MB-231 cells. Ni-NTA agarose was used to pull down His-β-catenin complex, following with SDS-PAGE and western blotting.

Mammary gland whole mount

No. 4 mammary glands were removed from *CD177^{-/-}* and *WT* mice and fixed in Carnoy's fix (six parts ethanol, three parts chloroform, and one-part glacial acetic acid) overnight. They were then rehydrated with ethanol washes, stained with carmine alum stain, cleared, and mounted. Whole-mount slides of mammary glands were marked an inch above the inguinal lymph node and all branch points within this inch were counted.

Immunohistochemistry

Tissues were processed with standard IHC protocols. Tris-based pH 9 antigen unmasking solution (Vector Labs) was used for antigen retrieval and samples were blocked with background punisher (BioCare Medical, Concord CA). Slides were incubated with primary antibody, anti Ki-67 antibody (D2H10; Cell signaling), anti-KRT5 antibody (Poly 19055; Biolegend, San Diego, CA), anti-active β-catenin (D13A1; Cell Signaling), anti-ERα (C-311; Santa Cruz Biotechnology, Dallas, Texas), or anti-PR (D8Q2J; Cell Signaling) for 2 h. Next, rabbit or mouse-on-rodent polymers (BioCare Medical) for 30 min, developed with 3,3'-diaminobenzidine (0.3% H₂O₂ in PBS) developing buffer, and counterstained. Positive cells and total cells per mammary duct were counted.

Immunofluorescence staining and confocal microscopy

Frozen tissue samples or plated cells were fixed for 20 min with 35% methanol/65% acetone on ice. The samples were rehydrated with ice-cold PBS, permeabilized, blocked with 5% goat serum and 0.3% Triton X-100, then incubated with primary antibodies, CD177 (Clone 4C4, Sigma Aldrich), β-catenin (H-102; Santa Cruz Biotechnology), or E-cadherin (DECMA-1; Santa Cruz Biotechnology) overnight. The slides were then counterstained with ToPro3 and SlowFade diamond antifade with DAPI (Life Technologies). Images were taken using a Zeiss LSM710 or LSM510 confocal microscope.

Luciferase assay

In all, 1×10^5 cells/well were plated in 24-well plates. After 24 h cells were transfected with pRL-RLuc-Myc (Promega,

Madison, WI) and M50 Super8x TOPflash (Addgene Plasmid # 12456) [45], plasmids at a 1:16 ratio. MDA-MB-436 were co-transfected with 500 ng CD177-myc, E-cadherin or empty pcDNA3 plasmids, alone or together. H146 cells were co-transfected with 25 nM CD177 or Non-targeting siRNAs (L-020431-00-0005, D-001810-10-20; Dharmacon, Lafayette, CO). 24 h after transfection, media was collected and 400 ng/mL recombinant Wnt3a (R&D Systems, Minneapolis, MN) or vehicle was added and distributed back to the cells. For 67NR cells, following transfection 1×10^5 cells were plated in polyHEMA coated 24-well plates for 24 h prior to treatment with Wnt3a. Luciferase levels were measured using the Dual-Luciferase Reporter Assay System (Promega, Madison, WI) 24 h after treatment. Sequence for *CD177* siRNA was as follows: ACACGUUGAUGCUCUAUGA, CAGUUCAGCAUGUGUGGAA, GCAACAACCUCGUUAACUC and GGACACCAUUAUGACACA.

Flow cytometry

Cells were suspended in PBS with 2% FBS and incubated with CD177-FITC conjugated antibody (MEM-166; Biolegend) for 30 min. Cells were washed and evaluated by flow cytometry using a BD FACSCanto II (BD Biosciences, San Jose, CA) and analyzed using FlowJo software (FlowJo LLC, Ashland, OR).

Real-time PCR

RNA was isolated as described above and cDNA was generated using Superscript III First Strand cDNA Synthesis Kit (Thermo Fisher Scientific). mRNA expression was quantified by real-time PCR using SYBR premix Ex Taq II (Takara, Mountain View, CA) and analyzed using ViiA7 Real-time PCR System (Thermo Fisher Scientific). The following primers were used: Human *CD177* F-CCAGGAGGACTTCTGCAACA R-ACTGGGCACCTCAAGGATCC, Mouse *Cd177* F-CCGGGAGAATATGGAGACAC, R-CGCTGCTGCTCATAGACGTA, Mouse *Lgr5* F-TCTTCTAGGAAGCAGAGGCG R-CAACCTCAGC GTCTTCACCT, Mouse *Axin2* F-TGCATCTCTCTGGAGCTG R-ACTGACCGACGATTCCATGT, Mouse *TCF4* F-TCTCCATAGTTCCCTGGACGG R-GTGGACATTTTAC TGGCTCA, Mouse *Fabp5* F-TGTTGTTGCCATCACACGTA R-CGGCTTTGAGGA GTACATGA, Mouse *Snai2* F-GATGTGCCCTCAGGTTTGAT R-GGCTGCTTCAA GGACACATT, Mouse *Sfrp1* F- GGGTTTCTTCTTCTTGGGGA R-CATCTCTGTGCAAGCGAGTT, Mouse *Il2rg* F-GAA CCC GAAATGTGTACCGT R-ACAGAGATCGAAGC TGGACG, Mouse *Ppia* F-CAGTGCTCAGA GCTC GAAAGT R-GTGTCTTCGACATCACGGC, Mouse

Ctnnb1 F- ATGGAGCCGGACAGAAAAGC R- CTTGCCACTCAGGGAAGGA.

CRISPR/Cas9

E-cadherin protein expression was knocked down using the LentiCRISPRv2 (Addgene plasmid #52961) CRISPR/Cas9 system [46, 47]. The guide sequence, 5'-ATAGGCTGTCTCTTTGTCGA-3', was ligated into the LentiCRISPRv2 plasmid using Roche Rapid Ligation kit (Basel, Switzerland). The lentiviral particles were packaged in HEK293T cells followed by infection of target cells. Puromycin was used for selection, followed by flow cytometry to sort out E-cadherin-negative population.

RNA sequencing and genomic analysis

RNA from tumor samples were isolated with RNeasy Plus Mini Kit (Qiagen, Hilden, Germany). Samples with an RNA Integrity Number score > 8.0 as measured by an Agilent BioAnalyzer 2100 were submitted to the University of Chicago Genomics. Paired-end 75 bp on the Illumina HiSeq 2000 was performed. Gene sets related to Wnt/ β -catenin signaling enriched in the *CD177*-low expressing groups with a false discovery rate < 0.25 were identified and graphed using Prism GraphPad software.

Raw data were aligned using the USeGalaxy web platform and TopHat with the mm10 genome [48–50]. The aligned bam files were further processed according to the previously established workflow for cufflinks [51] using quartile and bias corrections. Z scores were calculated using the resulting gene expression file and a heatmap of β -catenin-regulated genes was generated using Graphpad Prism Software (Graphpad Software Inc). Expression versus methylation analysis utilized mean-centralized level 3 Illumina HiSeq 2000 RNAseq expression data and Infinium HumanMethylation450 beta-values. Data were downloaded from the UCSC Cancer Genome Browser with samples being divided into primary tumor and paired normal tissue samples. Copy number analysis was done using cBioportal with the available cancer data sets [41, 42]. Expression data for Breast cancer (GSE2034), LUSC (TCGA), and COAD/READ (TCGA) were separated into groups with high and low expression of *CD177* and GSEA was performed using the Molecular Signature Database (MSigDB) [52, 53].

Statistical methods

Logrank testing was used to determine significance for all survival curves. One-way analysis of variance (ANOVA) with multiple comparisons was used to determine significance for dual-luciferase assays. Significance of tumor

growth curves was determined with two-way ANOVA. Significance for all other experiments was determined by Student's *t* test assuming equal variance. *P* values ≤ 0.05 were considered significant.

Acknowledgements W.Z. was supported by NIH grants CA200673 and CA203834, the V Scholar award, American Cancer Society seed grant, Breast Cancer Research Award and Oberley Award (National Cancer Institute Award P30CA086862) from Holden Comprehensive Cancer Center at the University of Iowa, University of Iowa. N.B. was supported by NIH CA206255. Q.X. was supported by the National Natural Science Foundation of China (No. 81502313). We thank Dr. Foekens for sharing the site-specific metastasis information related to GSE2034. We thank Dr. Shay for sharing the human colon epithelial cells.

Author contributions P.N.K., R.K., D.Z., X.S., and W.Z. conceived and designed the experiments. R.K. and Q.X. obtained the mouse tumor data. R.K., P.N.K., Q.X., Q.L.L., M.K., Y.L. did the biochemical studies. P.N.K., Y.L. performed the immunofluorescent staining, immunohistochemistry, and analysis of normal mammary gland. N.B. processed the RNAseq data and obtained methylation data. W.L., C.S., L.W., and A.W.T. provided technical support. A.B. provided TMAs and assigned IHC scores. K.N.G. and C.Z. provided histological help on tumor and tumor mammary tissues., S.S. and R.J. W. provided human breast cancer protein, RNA and tissue samples. R.K., P.N.K., X.S., D.Z., and W.Z. analyzed the data and wrote the manuscript. W.Z. supervised the whole project.

Compliance with ethical standards

Conflict of interest The authors declare that they have no conflict of interest.

Publisher's note Springer Nature remains neutral with regard to jurisdictional claims in published maps and institutional affiliations.

References

1. Temerinac S, Klippel S, Strunck E, Roder S, Lubbert M, Lange W, et al. Cloning of PRV-1, a novel member of the uPAR receptor superfamily, which is overexpressed in polycythemia rubra vera. *Blood*. 2000;95:2569–76.
2. Kissel K, Santoso S, Hofmann C, Stroncek D, Bux J. Molecular basis of the neutrophil glycoprotein NB1 (CD177) involved in the pathogenesis of immune neutropenias and transfusion reactions. *Eur J Immunol*. 2001;31:1301–9.
3. Caruccio L, Bettinotti M, Director-Myska AE, Arthur DC, Stroncek D. The gene overexpressed in polycythemia rubra vera, PRV-1, and the gene encoding a neutrophil alloantigen, NB1, are alleles of a single gene, CD177, in chromosome band 19q13.31. *Transfusion*. 2006;46:441–7.
4. Passamonti F, Pietra D, Malabarba L, Rumi E, Della Porta MG, Malcovati L, et al. Clinical significance of neutrophil CD177 mRNA expression in Ph-negative chronic myeloproliferative disorders. *Br J Haematol*. 2004;126:650–6.
5. Xie Q, Klesney-Tait J, Keck K, Parlet C, Borchering N, Kolb R, et al. Characterization of a novel mouse model with genetic deletion of CD177. *Protein Cell*. 2015;6:117–26.
6. Dalerba P, Kalisky T, Sahoo D, Rajendran PS, Rothenberg ME, Leyrat AA, et al. Single-cell dissection of transcriptional heterogeneity in human colon tumors. *Nat Biotechnol*. 2011;29:1120–7.
7. Toyoda T, Tsukamoto T, Yamamoto M, Ban H, Saito N, Takasu S, et al. Gene expression analysis of a *Helicobacter pylori*-infected and high-salt diet-treated mouse gastric tumor model: identification of CD177 as a novel prognostic factor in patients with gastric cancer. *BMC Gastroenterol*. 2013;13:122.
8. MacDonald BT, Tamai K, He X. Wnt/beta-catenin signaling: components, mechanisms, and diseases. *Dev Cell*. 2009;17:9–26.
9. Clevers H, Nusse R. Wnt/beta-catenin signaling and disease. *Cell*. 2012;149:1192–205.
10. Eger A, Stockinger A, Schaffhauser B, Beug H, Foisner R. Epithelial mesenchymal transition by c-Fos estrogen receptor activation involves nuclear translocation of beta-catenin and upregulation of beta-catenin/lymphoid enhancer binding factor-1 transcriptional activity. *J Cell Biol*. 2000;148:173–88.
11. Orsulic S, Huber O, Aberle H, Arnold S, Kemler R. E-cadherin binding prevents beta-catenin nuclear localization and beta-catenin/LEF-1-mediated transactivation. *J Cell Sci*. 1999;112:1237–45.
12. Kuphal F, Behrens J. E-cadherin modulates Wnt-dependent transcription in colorectal cancer cells but does not alter Wnt-independent gene expression in fibroblasts. *Exp Cell Res*. 2006;312:457–67.
13. Onder TT, Gupta PB, Mani SA, Yang J, Lander ES, Weinberg RA. Loss of E-cadherin promotes metastasis via multiple downstream transcriptional pathways. *Cancer Res*. 2008;68:3645–54.
14. Stockinger A, Eger A, Wolf J, Beug H, Foisner R. E-cadherin regulates cell growth by modulating proliferation-dependent beta-catenin transcriptional activity. *J Cell Biol*. 2001;154:1185–96.
15. Sanson B, White P, Vincent JP. Uncoupling cadherin-based adhesion from wingless signalling in *Drosophila*. *Nature*. 1996;383:627–30.
16. Heasman J, Ginsberg D, Geiger B, Goldstone K, Pratt T, Yoshida-Noro C, et al. A functional test for maternally inherited cadherin in *Xenopus* shows its importance in cell adhesion at the blastula stage. *Development*. 1994;120:49–57.
17. Gottardi CJ, Wong E, Gumbiner BM. E-cadherin suppresses cellular transformation by inhibiting beta-catenin signaling in an adhesion-independent manner. *J Cell Biol*. 2001;153:1049–60.
18. Fagotto F, Funayama N, Gluck U, Gumbiner BM. Binding to cadherins antagonizes the signaling activity of beta-catenin during axis formation in *Xenopus*. *J Cell Biol*. 1996;132:1105–14.
19. Incassati A, Chandramouli A, Eelkema R, Cowin P. Key signaling nodes in mammary gland development and cancer: beta-catenin. *Breast Cancer Res*. 2010;12:213.
20. Polakis P. The many ways of Wnt in cancer. *Curr Opin Genet Dev*. 2007;17:45–51.
21. Koesters R, Ridder R, Kopp-Schneider A, Betts D, Adams V, Niggli F, et al. Mutational activation of the beta-catenin proto-oncogene is a common event in the development of Wilms' tumors. *Cancer Res*. 1999;59:3880–2.
22. Chiurillo MA. Role of the Wnt/beta-catenin pathway in gastric cancer: an in-depth literature review. *World J Exp Med*. 2015;5:84–102.
23. Badders NM, Goel S, Clark RJ, Klos KS, Kim S, Bafico A, et al. The Wnt receptor, Lrp5, is expressed by mouse mammary stem cells and is required to maintain the basal lineage. *PLoS ONE*. 2009;4:e6594.
24. Lindvall C, Evans NC, Zylstra CR, Li Y, Alexander CM, Williams BO. The Wnt signaling receptor Lrp5 is required for mammary ductal stem cell activity and Wnt1-induced tumorigenesis. *J Biol Chem*. 2006;281:35081–7.
25. Lindvall C, Zylstra CR, Evans N, West RA, Dykema K, Furge KA, et al. The Wnt co-receptor Lrp6 is required for normal mouse mammary gland development. *PLoS ONE*. 2009;4:e5813.
26. Tepera SB, McCrea PD, Rosen JM. A beta-catenin survival signal is required for normal lobular development in the mammary gland. *J Cell Sci*. 2003;116:1137–49.
27. Brisken C, Heineman A, Chavarria T, Elenbaas B, Tan J, Dey SK, et al. Essential function of Wnt-4 in mammary gland

- development downstream of progesterone signaling. *Genes Dev.* 2000;14:650–4.
28. Chu EY, Hens J, Andl T, Kairo A, Yamaguchi TP, Briskin C, et al. Canonical Wnt signaling promotes mammary placode development and is essential for initiation of mammary gland morphogenesis. *Development.* 2004;131:4819–29.
 29. Zeng YA, Nusse R. Wnt proteins are self-renewal factors for mammary stem cells and promote their long-term expansion in culture. *Cell Stem Cell.* 2010;6:568–77.
 30. Teuliere J, Faraldo MM, Deugnier MA, Shtutman M, Ben-Ze'ev A, Thiery JP, et al. Targeted activation of beta-catenin signaling in basal mammary epithelial cells affects mammary development and leads to hyperplasia. *Development.* 2005;132:267–77.
 31. Zhang J, Li Y, Liu Q, Lu W, Bu G. Wnt signaling activation and mammary gland hyperplasia in MMTV-LRP6 transgenic mice: implication for breast cancer tumorigenesis. *Oncogene.* 2010;29:539–49.
 32. Imbert A, Eelkema R, Jordan S, Feiner H, Cowin P. Delta N89 beta-catenin induces precocious development, differentiation, and neoplasia in mammary gland. *J Cell Biol.* 2001;153:555–68.
 33. Tsukamoto AS, Grosschedl R, Guzman RC, Parslow T, Varmus HE. Expression of the int-1 gene in transgenic mice is associated with mammary gland hyperplasia and adenocarcinomas in male and female mice. *Cell.* 1988;55:619–25.
 34. Hayes MJ, Thomas D, Emmons A, Giordano TJ, Kleer CG. Genetic changes of Wnt pathway genes are common events in metaplastic carcinomas of the breast. *Clin Cancer Res.* 2008;14:4038–44.
 35. Ozaki S, Ikeda S, Ishizaki Y, Kurihara T, Tokumoto N, Iseki M, et al. Alterations and correlations of the components in the Wnt signaling pathway and its target genes in breast cancer. *Oncol Rep.* 2005;14:1437–43.
 36. Prasad CP, Gupta SD, Rath G, Ralhan R. Wnt signaling pathway in invasive ductal carcinoma of the breast: relationship between beta-catenin, dishevelled and cyclin D1 expression. *Oncology.* 2007;73:112–7.
 37. Khramtsov AI, Khramtsova GF, Tretiakova M, Huo D, Olopade OI, Goss KH. Wnt/beta-catenin pathway activation is enriched in basal-like breast cancers and predicts poor outcome. *Am J Pathol.* 2010;176:2911–20.
 38. Györfy B, Lanczky A, Eklund AC, Denkert C, Budczies J, Li Q, et al. An online survival analysis tool to rapidly assess the effect of 22,277 genes on breast cancer prognosis using microarray data of 1,809 patients. *Breast Cancer Res Treat.* 2010;123:725–31.
 39. Wang Y, Klijn JG, Zhang Y, Sieuwerts AM, Look MP, Yang F, et al. Gene-expression profiles to predict distant metastasis of lymph-node-negative primary breast cancer. *Lancet.* 2005;365:671–9.
 40. Minn AJ, Gupta GP, Siegel PM, Bos PD, Shu W, Giri DD, et al. Genes that mediate breast cancer metastasis to lung. *Nature.* 2005;436:518–24.
 41. Gao J, Aksoy BA, Dogrusoz U, Dresdner G, Gross B, Sumer SO, et al. Integrative analysis of complex cancer genomics and clinical profiles using the cBioPortal. *Sci Signal.* 2013;6:p11.
 42. Cerami E, Gao J, Dogrusoz U, Gross BE, Sumer SO, Aksoy BA, et al. The cBio cancer genomics portal: an open platform for exploring multidimensional cancer genomics data. *Cancer Discov.* 2012;2:401–4.
 43. Feng Q, Zhang Z, Shea MJ, Creighton CJ, Coarfa C, Hilsenbeck SG, et al. An epigenomic approach to therapy for tamoxifen-resistant breast cancer. *Cell Res.* 2014;24:809–19.
 44. Matsuzawa A, Tseng PH, Vallabhapurapu S, Luo JL, Zhang W, Wang H, et al. Essential cytoplasmic translocation of a cytokine receptor-assembled signaling complex. *Science.* 2008;321:663–8.
 45. Veeman MT, Slusarski DC, Kaykas A, Louie SH, Moon RT. Zebrafish prickles, a modulator of noncanonical Wnt/Fz signaling, regulates gastrulation movements. *Curr Biol.* 2003;13:680–5.
 46. Shalem O, Sanjana NE, Hartenian E, Shi X, Scott DA, Mikkelsen TS, et al. Genome-scale CRISPR-Cas9 knockout screening in human cells. *Science.* 2014;343:84–87.
 47. Sanjana NE, Shalem O, Zhang F. Improved vectors and genome-wide libraries for CRISPR screening. *Nat Methods.* 2014;11:783–4.
 48. Goecks J, Nekrutenko A, Taylor J, Galaxy T. Galaxy: a comprehensive approach for supporting accessible, reproducible, and transparent computational research in the life sciences. *Genome Biol.* 2010;11:R86.
 49. Blankenberg D, Von Kuster G, Coraor N, Ananda G, Lazarus R, Mangan M et al. Galaxy: a web-based genome analysis tool for experimentalists. *Curr Protoc Mol Biol* 2010; Chapter 19: Unit 19.10.1-21.
 50. Giardine B, Riemer C, Hardison RC, Burhans R, Elnitski L, Shah P, et al. Galaxy: a platform for interactive large-scale genome analysis. *Genome Res.* 2005;15:1451–5.
 51. Trapnell C, Roberts A, Goff L, Pertea G, Kim D, Kelley DR, et al. Differential gene and transcript expression analysis of RNA-seq experiments with TopHat and Cufflinks. *Nat Protoc.* 2012;7:562–78.
 52. Subramanian A, Tamayo P, Mootha VK, Mukherjee S, Ebert BL, Gillette MA, et al. Gene set enrichment analysis: a knowledge-based approach for interpreting genome-wide expression profiles. *Proc Natl Acad Sci USA.* 2005;102:15545–50.
 53. Liberzon A, Subramanian A, Pinchback R, Thorvaldsdottir H, Tamayo P, Mesirov JP. Molecular signatures database (MSigDB) 3.0. *Bioinformatics.* 2011;27:1739–40.
 54. Uhlen M, Zhang C, Lee S, Sjöstedt E, Fagerberg L, Bidkhorji G et al. A pathology atlas of the human cancer transcriptome. *Science* 2017; 357:pii: eaan2507.
 55. Borcherding N, Cole K, Kluz P, Jorgensen M, Kolb R, Bellizzi A, et al. Re-evaluating E-cadherin and beta-catenin: a pan-cancer proteomic approach with an emphasis on breast cancer. *Am J Pathol.* 2018;188:1910–20.
 56. Geyer FC, Lacroix-Triki M, Savage K, Arnedos M, Lambros MB, MacKay A, et al. beta-catenin pathway activation in breast cancer is associated with triple-negative phenotype but not with CTNNB1 mutation. *Mod Pathol.* 2011;24:209–31.
 57. Bulut G, Fallen S, Beauchamp EM, Drebing LE, Sun J, Berry DL, et al. Beta-catenin accelerates human papilloma virus type-16 mediated cervical carcinogenesis in transgenic mice. *PLoS ONE.* 2011;6:e27243.
 58. Chen Q, Cao HZ, Zheng PS. LGR5 promotes the proliferation and tumor formation of cervical cancer cells through the Wnt/beta-catenin signaling pathway. *Oncotarget.* 2014;5:9092–105.
 59. Zhang YN, Liu BZ, Zhao QY, Hou T, Huang X. Nuclear localization of beta-catenin is associated with poor survival and chemo-/radioresistance in human cervical squamous cell cancer. *Int J Clin Exp Pathol.* 2014;7:3908–17.
 60. Kypta RM, Waxman J. Wnt/beta-catenin signalling in prostate cancer. *Nat Rev Urol.* 2012;9:418–28.
 61. Yokoyama NN, Shao S, Hoang BH, Mercola D, Zi X. Wnt signaling in castration-resistant prostate cancer: implications for therapy. *Am J Clin Exp Urol.* 2014;2:27–44.
 62. Nakashima N, Liu D, Huang CL, Ueno M, Zhang X, Yokomise H. Wnt3 gene expression promotes tumor progression in non-small cell lung cancer. *Lung Cancer.* 2012;76:228–34.
 63. Uematsu K, He B, You L, Xu Z, McCormick F, Jablons DM. Activation of the Wnt pathway in non small cell lung cancer: evidence of dishevelled overexpression. *Oncogene.* 2003;22:7218–21.